JOURNAL OF AIRCRAFT
Vol. 40, No. 3, May–June 2003

Analysis of Nonlinear Aeroelastic Signals

Hekmat Alighanbari*
Ryerson University, Toronto, Ontario M5B 2K3, Canada
and
B. H. K. Lee†
National Research Council, Ottawa, K1A 0R6 Canada

A signal processing technique is presented to analyze nonlinear aeroelastic time series where limit-cycle oscillations and chaotic motions may occur. A powerful method to study nonlinear aeroelastic behavior of aircraft structures is the phase-space reconstruction technique. In the reconstruction process, the mutual information function and the percentage of false neighbors methods are used to estimate the time delay and the dimension of the attractor, respectively. The dynamics of the system are then determined from the Lyapunov exponents. A method of estimating frequency and damping values of the aeroelastic system from the reconstructed phase space is also presented. Examples are given for a two-dimensional airfoil oscillating in pitch and plunge with either a bilinear or a cubic spring nonlinearity in one of the degrees of freedom.

Nomenclature

a_h	=	nondimensional distance from airfoil midchord to elastic axis
b	=	airfoil semichord
d_e	=	embedding dimension
K_c	=	central stiffness term for the bilinear stiffness
M	=	nonlinear structural restoring moment
M_0	=	restoring moment at the start of the central bilinear stiffness
m	=	airfoil mass
p	=	nondimensional aerodynamic force in the plunge direction
r	=	nondimensional aerodynamic pitching moment
r_α	=	radius of gyration about elastic axis
T	=	time delay
U^*	=	nondimensional freestream velocity, $V/b\omega_\alpha$
U_L^*	=	nondimensional linear flutter velocity
V	=	freestream velocity
x	=	scalar time history at discrete time intervals
x_α	=	nondimensional distance from elastic axis to center of mass
$\boldsymbol{y}$	=	finite vector sampled from x scalar time history
α	=	pitch angle of the airfoil
α_f	=	α at the start of the freeplay
δ	=	pitch angle for the central region of the bilinear stiffness
ζ_ξ, ζ_α	=	viscous damping ratios in plunge and pitch
μ	=	airfoil/air mass ratio, $m/\pi\rho b^2$
ξ	=	nondimensional plunge displacement, h/b
τ	=	nondimensional time, tV/b
ω_ξ, ω_α	=	circular frequencies in plunge and pitch
$\bar{\omega}$	=	frequency ratio, ω_ξ/ω_α

Received 17 May 2001; revision received 20 June 2002; accepted for publication 18 August 2002.

*Assistant Professor, Department of Mechanical, Aerospace and Industrial Engineering; halighan@ryerson.ca. Member AIAA.

†Principal Research Officer, Institute for Aerospace Research, Aerodynamics Laboratory. Associate Fellow AIAA.

Introduction

FOR attached low-speed flow and small structural deformation, one can approximate the response of an aircraft structure to perturbations using a linear approach. However, there arise many situations where a linear approximation is not applicable and one has to take into consideration nonlinearities that can substantially modify the response behavior while at the same time make the analysis much more difficult. In fluid–structure interaction problems, the nonlinearities could arise from the fluid motion or from the structural properties. One of the most important aspects of nonlinear behavior in aeroelasticity is the appearance of limit-cycle oscillations (LCOs) and, under certain conditions, chaotic motions. The most easily recognized characteristic of LCOs is a sustained periodic motion of a wing, control surface, or an underwing store. The amplitude of motion can be constant, or in some cases it can fluctuate between limits that are not very far apart. LCOs are undesirable because they can cause structural fatigue, and they can also degrade the weapon platform of combat aircraft. In addition, vibrations at the pilot's seat can induce human fatigue and decrease the operational effectiveness of the pilot.

To date, most research efforts in nonlinear aeroelasticity have been dedicated to use nonlinear dynamics theory to gain a better understanding and interpretation of complex aeroelastic behavior. A review on these efforts was recently given by Lee et al.[1] The present study tends to explore advantages of nonlinear dynamics theory in the analysis of nonlinear time series arising from aeroelastic systems. Theories and techniques such as phase-space reconstruction have been developed by nonlinear dynamicists for the analysis of nonlinear time series. These theories and some of their applications are described in the recent monograph by Abarbanel.[2] This paper gives a brief description of the phase-space reconstruction technique[2] applied to aeroelastic systems and gives some sample results for LCOs obtained for a two-degree-of-freedom airfoil motion with structural nonlinearity parameters similar to those considered by Lee et al.[1]

Nonlinear Aeroelastic Signal Processing

A feature of LCOs in aeroelastic systems is that under certain conditions LCOs can change to chaotic motion through frequency doubling or quasi-periodic bifurcations. In such a case, the vibration signals resemble random signals, and the usual flutter parameter identification tools based on linear signal processing techniques will not be adequate. Thus, one needs to have some reliable means to analyze nonlinear response signals having decaying, periodic, or chaotic characteristics. There are various suggested approaches on this subject, such as wavelets and neural networks.[3] Amongst the various

methods available, the phase-space reconstruction technique[2] used by nonlinear dynamicists offers a great potential in flutter signal analysis.

In any signal processing technique, first the signal should be prepared for the analysis. In a linear case, one may enhance the signal by passing it through a filter. However, in the nonlinear dynamics approach, the process favored by nonlinear dynamicists is to use manifold decomposition.[2] After the signal preparation, the usual linear approach is to perform a Fourier transformation and power spectral analysis. However, for a nonlinear system with possibly chaotic behavior, power spectral density may not be a reliable tool to determine the real structural modes of the system. In a nonlinear dynamics approach, the counterpart to the power spectral analysis is to carry out a phase-space reconstruction to find the space or embedding dimension. Finally, a linear signal can be classified by its spectral properties; whereas, in the nonlinear case, the Lyapunov exponents or the fractal dimensions are used for this purpose.

The time series of the response can be obtained experimentally by placing sensors such as accelerometers or strain gauges on the aircraft structure. The signals are digitally sampled, and they are scalar quantities designated by $x(n)$, where n is the sample number that can be converted to time once the sampling frequency is given. To construct the phase space, one would typically need to obtain the position and velocity of the system at various time t. However, the main idea in the present analysis is that one does not need to measure both variables to capture the structure of the orbit of the phase curves. When started from the observed scalar quantity $x(n)$, the state space vector $\boldsymbol{y}(n)$ could be formed in d_e-dimensional space using a time delay T,

$$\boldsymbol{y}(n) = [x(n), x(n+T), x(n+2T), \ldots, x(n+(d_e-1)T)] \qquad n = 1, 2, 3, \ldots, N \quad (1)$$

Plotting this vector in a d_e-dimensional space represents the phase space of the system, for example, $\boldsymbol{y}(n) = [x(n), x(n+T)]$ and $\boldsymbol{y}(n) = [x(n), x(n+T), x(n+2T)]$ give a two-dimensional and three-dimensional phase space, respectively.

The key point in the time-delay reconstruction method is that all variables are connected in a nonlinear process. For example, $x(n)$ and $x(n+T)$ are related by the evolution of the dynamic system over a time interval T during which all dynamic variables affect the observed variable $x(n)$. Therefore, $x(n+T)$ is a complicated, unknown, nonlinear combination of all variables of the system. Alone, it may represent one of the variables, but the combination into a d_e-dimensional vector of time delays of $x(n)$ represents d_e active variables of the system being observed. If the time delay is too short, not enough time will elapse for the system to produce information about its dynamics. If it is too large, too much information will be lost, and the two data samples will not be correlated. The optimum time delay can be obtained using the average mutual information function.[4–6] The average mutual information identifies how much information regarding the state of the dynamic system, such as position or velocity, one can learn about a measurement at one time, $x(n+T)$, from a measurement taken at another time, $x(n)$. The expression for the mutual information $I(T)$ is given by

$$I(T) = \sum_{n=1}^{N} P[x(n), x(n+T)] \log_2 \left\{ \frac{P[x(n), x(n+T)]}{P[x(n)].P[x(n+T)]} \right\} \quad (2)$$

where $P[x(n)]$ and $P[x(n+T)]$ are, respectively, the probabilities of $x(n)$ and $x(n+T)$ occurring in the data set and $P[x(n), x(n+T)]$ is the joint probability. N is the total number of observed variable $x(n)$. The value of time delay T at which the first minimum of the mutual information occurs is then judged as the appropriate time delay to be used in the phase-space reconstruction technique. If the average mutual information has no minimum, it is recommended[5] to use T such that $I(T)/I(0)$ is approximately $\frac{1}{5}$. When T is selected using the described methods, the values of $x(n)$ and $x(n+T)$ contain useful information about its dynamics, while at the same time the two data samples are correlated.

To reconstruct the phase space one also needs to determine the dimension of the phase space or so called "embedding dimension." To find the embedding dimension d_e, the method of false nearest neighbors[6,7] is used in the present analysis. In this method, first the state space is reconstructed in a dimension d_e, and the Euclidean distances between each point and its nearest neighboring points in the reconstructed state space are calculated. The distance between point $\boldsymbol{y}(n)$ and its rth nearest neighbor, $\boldsymbol{y}^r(n)$, is calculated from

$$R^2_{de}(n, r) = \sum_{k=0}^{de-1} [x(n+kT) - x^r(n+kT)]^2, \qquad r = 1, 2, \ldots, N_b \quad (3)$$

Then, the process is repeated in a space dimension $d_e + 1$,

$$R^2_{de+1}(n, r) = R^2_{de}(n, r) + [x(n + d_eT) - x^r(n + d_eT)]^2 \qquad r = 1, 2, \ldots, N_b \quad (4)$$

If $\boldsymbol{y}^r(n)$ is a true neighbor, then it arrives at the neighborhood of $\boldsymbol{y}(n)$ in the state space through dynamic origins. It is a false neighbor if it arrives in the neighborhood of $\boldsymbol{y}(n)$ because the present dimension did not fully unfold the attractor, and when the embedding dimension is increased to $d_e + 1$, it is possible to move $\boldsymbol{y}^r(n)$ out of the neighborhood of $\boldsymbol{y}(n)$. The $\boldsymbol{y}(n)$ and $\boldsymbol{y}^r(n)$ are considered neighbors if the distance between them stays within a tolerance R_{tol} when the embedding dimension is increased from d_e to $d_e + 1$. The criterion for designating a neighbor to be false is given by Kennel et al.[7] as follows:

$$\left[\frac{R^2_{de+1}(n, r) - R^2_{de}(n, r)}{R^2_{de}(n, r)} \right]^{\frac{1}{2}} = \frac{\left| x(n + d_eT) - x^r(n + d_eT) \right|}{R_{de}(n, r)} > R_{\text{tol}} \quad (5)$$

Kennel et al.[7] suggest $R_{\text{tol}} > 10$, but in practice the final result does not change if R_{tol} is in the range $10 < R_{\text{tol}} < 50$. Once the percentage of false neighbors falls below some specified limit, then the corresponding dimension may be chosen as a sufficient embedding dimension. Kennel et al.[7] suggest the limit to be 1%.

For the case of a finite amount of data, the preceding criterion is not always sufficient to differentiate between close and nearest neighbors.[5] To resolve this problem, a second criterion is suggested as

$$R_{de+1}(n, r)/R_A > 2 \quad (6)$$

where R_A is the approximate size of the attractor defined by

$$R^2_A = \frac{1}{N} \sum_{n=1}^{N} [x(n) - x_{\text{av}}]^2, \qquad x_{\text{av}} = \frac{1}{N} \sum_{n=1}^{N} x(n) \quad (7)$$

Equation (6) implies that by increasing the embedding dimension by one a false neighbor will be displaced, in comparison to the size of the attractor, by a relatively large distance from its neighborhood in the state space.

Figure 1 shows the concept of phase-space reconstruction. Consider a set of available data, $x(n)$ representing an attractor of a system. Figure 1a shows the data projected on a one-dimensional space. In Fig. 1a, points indicating various states of the system can be at the same location on the axis, and Fig. 1a does not demonstrate much about the system's attractor. Figures 1b and 1c show the same data set projected on two- and three-dimensional spaces, respectively. Figures 1b and 1c give a better representation of the attractor. The definition of nearest neighbor is presented in Fig. 1b, where the first, second, and third neighbors of a typical point $\boldsymbol{y}(n)$ are indicated. The circles centered at point $\boldsymbol{y}(n)$ demonstrate the distances of these neighbors from $\boldsymbol{y}(n)$. Two points A and B in two-dimensional space may appear to be very close neighbors. However, these points are false neighbors because the reconstructed phase space in three

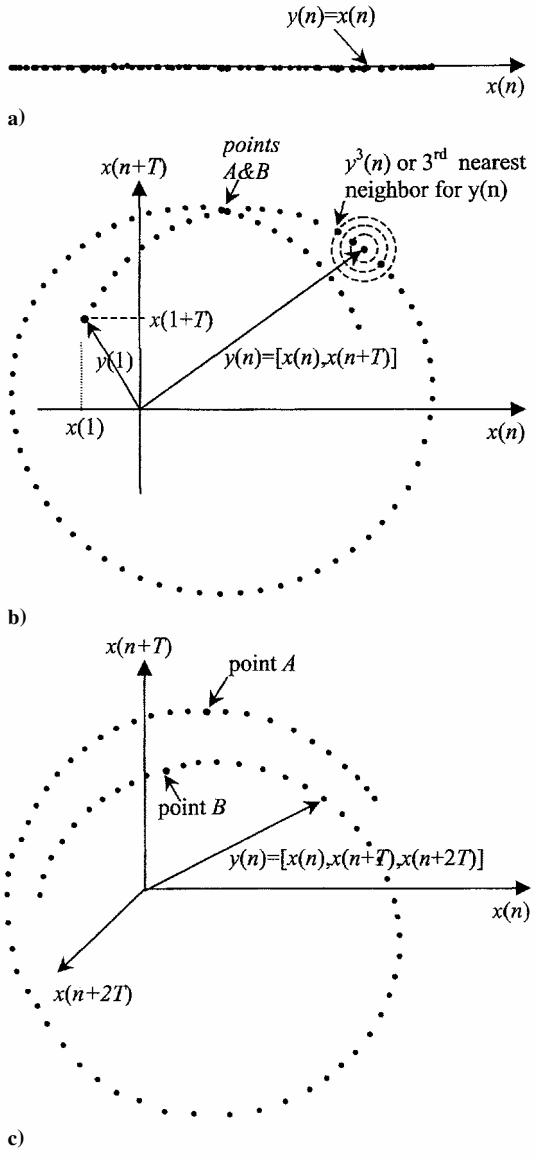

Fig. 1 Schematic of phase-space reconstruction.

dimensions separates the two points, and the distance between them is increased substantially in Fig. 1c. If the attractor is reconstructed in a four-dimensional space and all of the neighboring points in three dimensions remain neighbors in the four-dimensional space, then the minimum required embedding dimension would be three, $d_e = 3$, and Fig. 1c would represent the completely unfolded attractor.

After reconstructing the phase-space, one should be able to classify the dynamic system by finding the invariants of the system. Eigenvalues are the invariants for a linearized system. For a nonlinear system, Lyapunov exponents are the most important invariants. To determine the exponents, one may use the evolution of the state-space vector given by[8–10]

$$\boldsymbol{y}(n+T) = F[\boldsymbol{y}(n)] \tag{8}$$

This is the governing map for the reconstructed orbit. Function F is not known in algebraic form, but locally it can be estimated from the reconstructed space. At each point on the orbit $\boldsymbol{y}(n)$, a Taylor series for $F[\boldsymbol{y}(n)]$ is constructed in the vicinity of the orbit, and the Taylor series coefficients are determined numerically by a least-square fit to the data. The Taylor expansion order n_0 is a parameter to choose in this process. The expansion order depends on the structure of the attractor. One way to determine the appropriate order is simply to look at how accurately the calculated map fits the data and to increase n_0 to the point where the curvature of Taylor series can follow the curvature of the local data points quite closely.[10]

Small perturbations to the orbit evolve according to the linearized dynamics

$$\Delta\boldsymbol{y}(n+T) = DF(n)\Delta\boldsymbol{y}(n) \tag{9}$$

where $DF(n)$ is the Jacobian matrix of the map $F(n)$ at location $\boldsymbol{y}(n)$ on the orbit. The Jacobian matrices can be approximated from the linear term of the calculated Taylor series for $F[\boldsymbol{y}(n)]$. Once the Jacobian matrix of the mapping $F[\boldsymbol{y}(n)]$ for each point in the state space is known, one can use the multiplicative ergodic theorem of Oseledec[11] to determine the Lyapunov exponents of the system. When it is assumed that $DF^L(n)$ is the product of the Jacobian matrices L step along the orbit starting at location $y(n)$, that is, $DF^L(n) = DF(n+L-1)\cdot DF(n+L-2)\ldots DF(n+1)\cdot DF(n)$, where the dots represent matrix multiplication, the theorem states that if one forms the Oseledec matrix

$$\mathrm{OSL}(n, L) = \{[DF^L(n)]^T \cdot DF^L(n)\}^{1/2L} \tag{10}$$

then the limit of this matrix as $L \to \infty$ exists, and it is independent of $\boldsymbol{y}(n)$. Lyapunov exponents are simply the logarithm of the eigenvalues of this matrix when $L \to \infty$. Details of the procedure may be found in the paper by Wolf et al.[12]

After calculating the Jacobian matrix, one may adapt the following methodology to calculate the linearized modal damping and frequencies of the system. The linearized dynamic system is represented by $\dot{\boldsymbol{y}}(t) = [A]\boldsymbol{y}(t)$, where matrix $[A]$ determines the system dynamics and can be related to the Jacobian matrix as follows. The solution to $\dot{\boldsymbol{y}}(t) = [A]\boldsymbol{y}(t)$ can be written as $\boldsymbol{y}(n) = \exp([A]n\Delta t)\boldsymbol{y}_0$. Based on this exponential representation, a space perturbation $\Delta\boldsymbol{y}$ will evolve according to the expression

$$\Delta\boldsymbol{y}(n+T) = \exp([A]T\Delta t)\Delta\boldsymbol{y}(n) \tag{11}$$

Comparing Eq. (11) with Eq. (9) gives the relationship between $[A]$ and the Jacobian matrix

$$\exp([A]T\Delta t) = DF(n) \tag{12}$$

The Jacobian matrix depends on location in the phase space and, hence, the term $\exp([A]T\Delta t)$ obtained numerically will not be constant for every state vector in the phase space. However, they can be averaged to obtain a mean $\exp([A]T\Delta t)$ matrix, and the average complex exponents $\lambda_{1\mathrm{cplx}}, \lambda_{2\mathrm{cplx}}, \ldots, \lambda_{\mathrm{decplx}}$. These exponents are the eigenvalues of logarithm of the averaged matrix divided by $T\Delta t$. When the complex exponents are known, the frequency and damping values of the system can be obtained from the following expressions:

$$\zeta_i = \frac{\mathrm{Re}(\lambda_{i\,\mathrm{cplx}})}{\sqrt{[\mathrm{Re}(\lambda_{i\,\mathrm{cplx}})]^2 + [\mathrm{Im}(\lambda_{i\,\mathrm{cplx}})]^2}} \tag{13}$$

$$\omega_i = \frac{\mathrm{Re}(\lambda_{i\,\mathrm{cplx}})}{2\pi\zeta_i} \tag{14}$$

Results and Discussion

As an example to illustrate the procedure just outlined to reconstruct a phase space, some results for the pitch motion of a two-dimensional airfoil are presented herein. The airfoil, shown in Fig. 2, is placed in an incompressible flow and is free to oscillate in the pitch and plunge directions. Either a bilinear or cubic nonlinearity is considered in the pitch stiffness.

The equations of motion for the system may be written in nondimensional form as[1]

$$\xi''(\tau) + x_\alpha\alpha''(\tau) + 2\zeta_\xi(\bar{\omega}/U^*)\xi'(\tau) + (\bar{\omega}/U^*)^2\xi(\tau) = p(\tau)$$

$$\left(x_\alpha/r_\alpha^2\right)\xi''(\tau) + \alpha''(\tau) + 2\zeta_\alpha(1/U^*)\alpha'(\tau) + (1/U^{*2})M(\alpha) = r(\tau) \tag{15}$$

where α and ξ are the nondimensional pitch and heave displacements, respectively, of the airfoil measured at its elastic axis. $M(\alpha)$

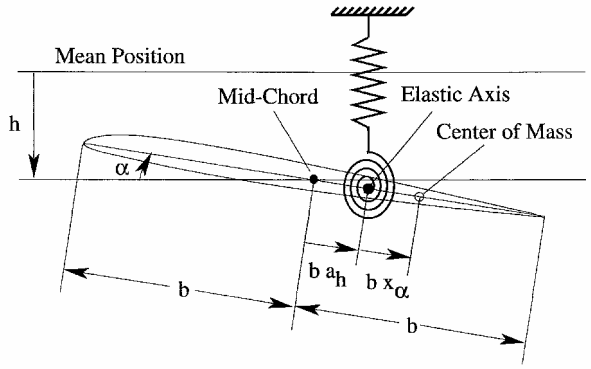

Fig. 2 Schematic representation of the two-degree-of-freedom airfoil.

is the structural nonlinearity in pitch, normalized with respect to the linear torsional stiffness. [In the case of a linear system, $M(\alpha)$ is simply α.] U^* is nondimensional airspeed, $(\,)'$ denotes differentiation with respect to nondimensional time τ, and the other symbols are defined in the Nomenclature. Here $p(\tau)$ and $r(\tau)$ are the nondimensional force and moment, respectively, including aerodynamic and other possible excitation forces. For incompressible flow, the unsteady aerodynamic force and moment in $p(\tau)$ and $r(\tau)$ for any arbitrary motion are given by[13]

$$p(\tau) = -\frac{1}{\mu}\left[\xi''(\tau) - a_h\alpha''(\tau) + \alpha'(\tau)\right] - \frac{2}{\mu}\left\{\left[\xi'(0) + \left(\frac{1}{2} - a_h\right)\alpha'(0) + \alpha(0)\right]\phi(\tau) + \int_0^\tau \left[\xi''(\sigma) + \left(\frac{1}{2} - a_h\right)\alpha''(\sigma) + \alpha'(\sigma)\right]\phi(\tau - \sigma)\,\mathrm{d}\sigma\right\} \tag{16}$$

$$r(\tau) = \frac{1}{\mu r_\alpha^2}\left[a_h\xi''(\tau) - \left(\frac{1}{8} + a_h^2\right)\alpha''(\tau) - \left(\frac{1}{2} - a_h\right)\alpha'(\tau)\right] + \frac{2}{\mu r_\alpha^2}\left(\frac{1}{2} + a_h\right)\left\{\left[\xi'(0) + \left(\frac{1}{2} - a_h\right)\alpha'(0) + \alpha(0)\right]\phi(\tau) + \int_0^\tau \left[\xi''(\sigma) + \left(\frac{1}{2} - a_h\right)\alpha''(\sigma) + \alpha'(\sigma)\right]\phi(\tau - \sigma)\,\mathrm{d}\sigma\right\} \tag{17}$$

where $\phi(\tau) = 1 - 0.165e^{-0.0455\tau} - 0.335e^{-0.3\tau}$ is the Wagner's function using the coefficients given by Jones.[14]

The specific structural nonlinearities considered in the following analysis are bilinear and cubic restoring moments in the pitch degree of freedom, as shown schematically in Fig. 3.

For the preceding system with either bilinear or cubic nonlinearity, LCOs can be obtained for velocities well below the linear flutter speed. For a given set of parameters, the airfoil can also experience chaotic oscillations through frequency doubling bifurcations for some range of airspeed.[15,16]

For the airfoil with bilinear nonlinearity, a two-dimensional phase-space plot of the α motion is shown in Fig. 4 with airfoil parameters $\bar{\omega} = 0.2$, $\mu = 100$, $a_h = -0.5$, $x_\alpha = 0.25$, $r_\alpha^2 = 0.25$, $\alpha_f = 0.25$ deg, $\delta = 0.5$ deg, $M_0 = 0$, $K_c = 0$, and $U^*/U_L^* = 0.3$. Figure 4 shows α' as a function of α, where α' is obtained from numerical simulation of Eq. (15). When the nonlinear signal processing technique described earlier is used, the phase space can also be constructed from measurements of α alone. The time delay required for phase-space reconstruction is obtained using the mutual information method. The mutual information $I(T)$ is determined from Eq. (2), and its variation with time delay is shown in Fig. 5.

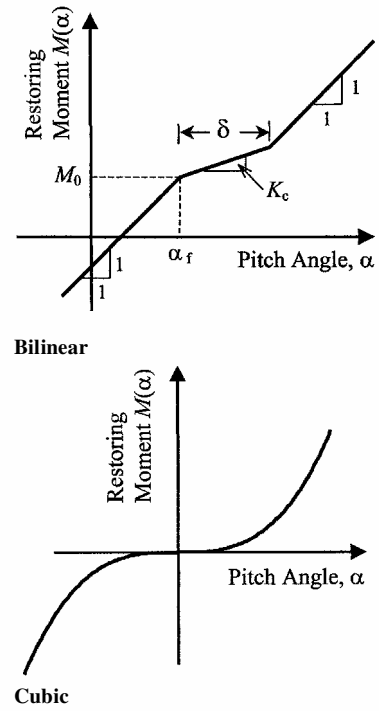

Fig. 3 Schematic of the structural nonlinearities.

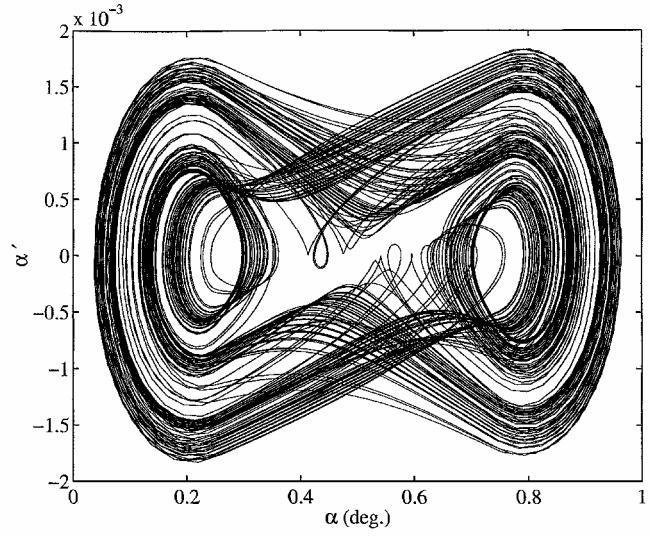

Fig. 4 Phase space of the pitch response for the airfoil with bilinear nonlinearity with $\bar{\omega} = 0.2$, $\mu = 100$, $a_h = -0.5$, $x_\alpha = 0.25$, $r_\alpha^2 = 0.25$, $\alpha_f = 0.25$ deg, $\delta = 0.5$ deg, $M_0 = 0$, and $U^*/U_L^* = 0.3$.

Figure 5 shows that, for small time delays $T < 5$, the mutual information is rather high. That is, reconstructed phase space with such time delays will not be fully unfolded because the coordinates $x(n)$ and $x(n+T)$ are too related to each other. In other words, not enough time elapsed between $x(n)$ and $x(n+T)$ for the system dynamics to affect $x(n+T)$ fully. On the other hand, time delays should not be so long that $x(n)$ and $x(n+T)$ become unrelated. The best time delay for phase-space reconstruction is $T = 10$, at which the first minimum of the $I(T)$ occurs. Time-delay coordinates, $x(n)$ and $x(n+T)$, are then used to reconstruct the phase space of the observed data, $x(n)$. Figure 6 shows the reconstructed phase space using $T = 10$. Compared with Fig. 4, it shows that the basic structure of the chaotic attractor has been captured.

Another example for a cubic nonlinearity is shown in Figs. 7 and 8 with airfoil parameters $\bar{\omega} = 0.2$, $\mu = 200$, $a_h = -0.5$, $x_\alpha = 0.25$, $r_\alpha^2 = 0.25$, and $M(\alpha) = 0.01\alpha + 50\alpha^3$. This system has rather interesting dynamics with a period doubling route to chaos.[16] Figure 7 shows a phase-plane plot of the system at $U^*/U_L^* = 0.475$ from

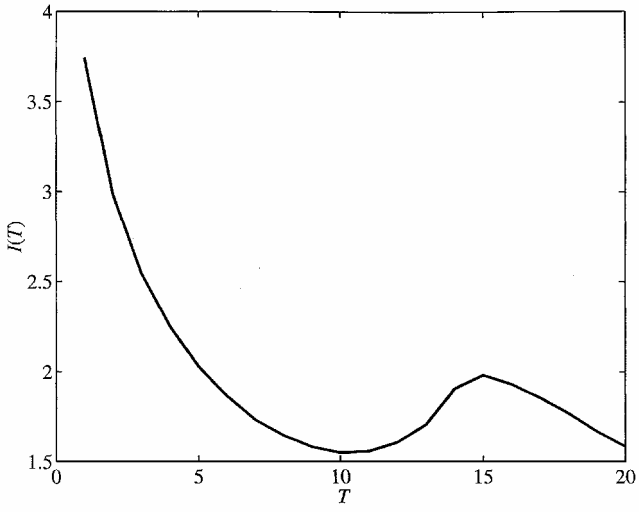

Fig. 5 Variation of the mutual information with nondimensional time delay for the pitch response of the airfoil with bilinear nonlinearity.

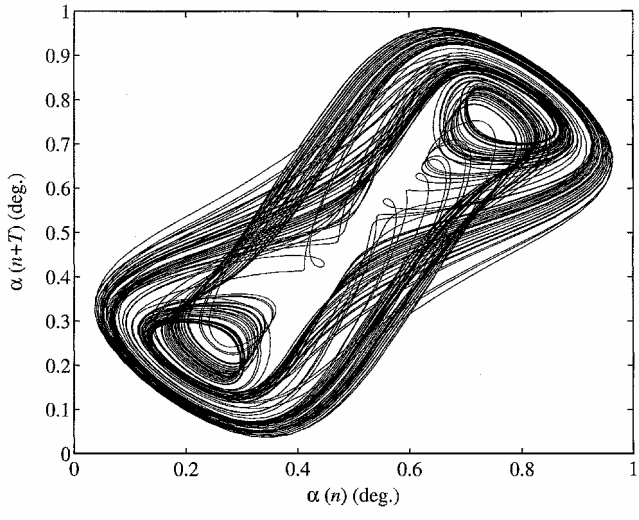

Fig. 6 Reconstructed phase space of the airfoil motion for the airfoil with bilinear nonlinearity and $T = 10$.

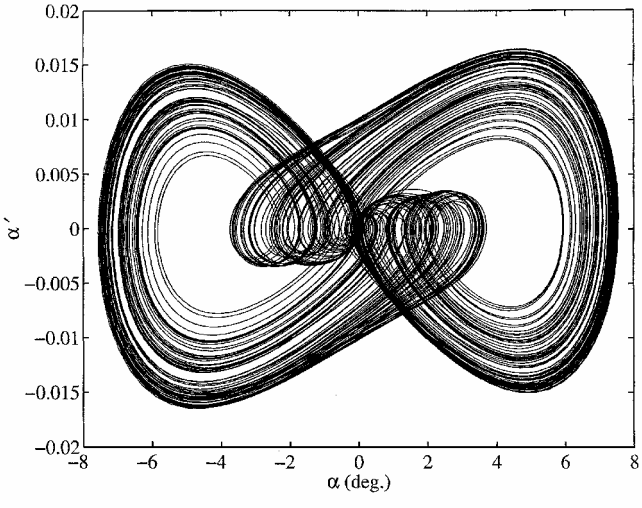

Fig. 7 Phase space of the pitch response for the airfoil with cubic nonlinearity with $\bar{\omega} = 0.2$, $\mu = 200$, $a_h = -0.5$, $x_\alpha = 0.25$, $r_\alpha^2 = 0.25$, $M(\alpha) = 0.01\alpha + 50\alpha^3$, and $U^*/U_L^* = 0.475$.

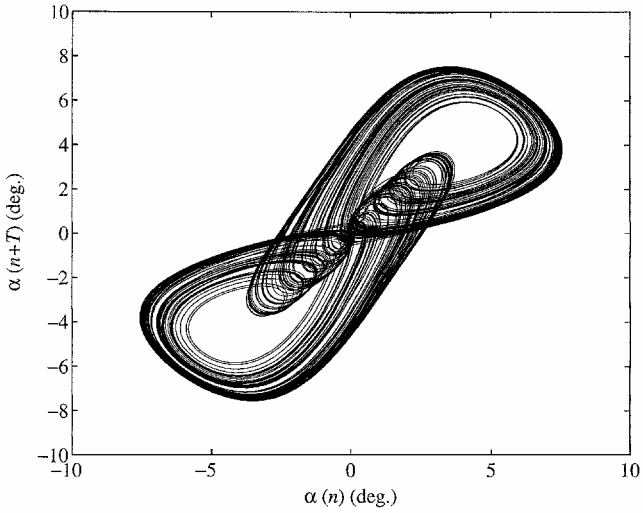

Fig. 8 Reconstructed phase space of the airfoil motion for the airfoil with cubic nonlinearity.

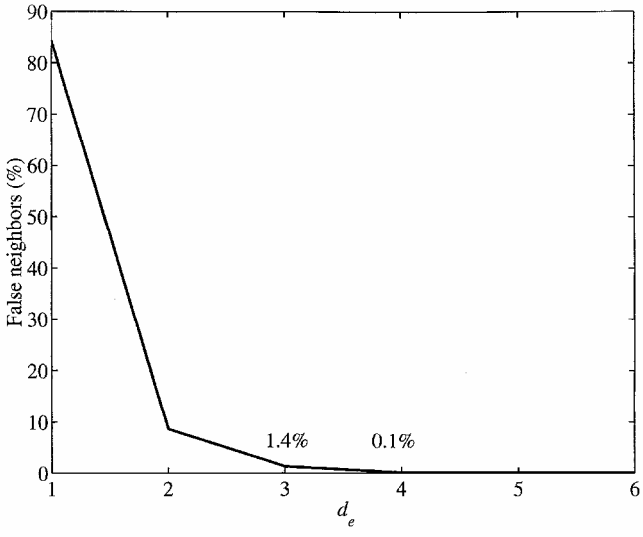

Fig. 9 Variation of percentage of false nearest neighbors with embedding dimension for the airfoil with bilinear nonlinearity and airspeed $U^*/U_L^* = 0.3$.

numerical integration of Eq. (15), and Fig. 8 is the reconstructed phase space. Again, the essential features of the system dynamics are captured from the nonlinear aeroelastic signal processing method presented earlier. Note that in the present analysis linear restoring hinge moment is defined as $M(\alpha) = \alpha$, and the linear flutter speed based on this definition and the preceding set of parameters is $U_L^* = 8.737$.

The false nearest neighbors[7] method was employed to calculate the minimum required embedding dimension of the described chaotic attractors. Figure 9 shows the variation of false nearest neighbors with the embedding dimension for the attractor illustrated in Fig. 6. As shown in Fig. 9, increasing the embedding dimension from 1 to 3 reduces the number of false neighbors from 84 to 1.4%. Figure 9 shows a sufficient embedding dimension of 4 at which the number of false neighbors is less than 1%. A similar result was obtained for the reconstructed attractor of Fig. 8 for the case of cubic nonlinearity.

The Lyapunov exponents were calculated using the method of Briggs[8] for the airfoil with cubic nonlinearity and the reconstructed attractor shown in Fig. 8. An embedding dimension of four was obtained from the method of false nearest neighbors and was used in the Lyapunov exponent calculation. For an analytical nonlinearity such as the cubic nonlinearity, it is also possible to calculate the Lyapunov exponents directly from the equations of motion. For this

purpose, the algorithm given by Wolf et al.[12] was used to calculate the complete Lyapunov spectrum from the differential equations.

The agreement between the Lyapunov exponents obtained directly from the equations of motion and those obtained from the reconstructed phase space is reasonably good, at least for the largest exponent, which is the one that indicates whether or not the system is chaotic. For example, when the pitch response from the airfoil with cubic nonlinearity shown in Fig. 7 is considered, the analytical solution gives a value of 0.008 for the largest exponent.[16] When the reconstructed data are used, the largest exponent varies between 0.007 and 0.01, depending on the Taylor expansion order n_0 and number of data points N_d used.

Lyapunov exponents are also calculated for the airfoil with bilinear nonlinearity and the reconstructed attractor shown in Fig. 6. When an embedding dimension of four obtained from the false nearest neighbors method is used, the largest positive exponent for this attractor is approximately 0.01, which is in good agreement with the values previously computed by Alighanbari and Price.[15]

An example using the earlier methodology for the calculation of damping ratios and frequencies for a linear dynamic system follows. In the absence of fluid motion, Eq. (15) can be reduced to a set of coupled equations for a mechanical system as

$$\xi'' + x_\alpha \alpha'' + 2\zeta_\xi \bar{\omega}\xi' + \bar{\omega}^2 \xi = 0$$

$$\left(x_\alpha / r_\alpha^2\right)\xi'' + \alpha'' + 2\zeta_\alpha \alpha' + \alpha = 0 \tag{18}$$

When Eqs. (18) were used, a time series of the ξ motion was obtained for the following parameters: $\bar{\omega} = 0.2$, $x_\alpha = 0.25$, $r_\alpha^2 = 0.25$, $\zeta_\xi = 0.01$, and $\zeta_\alpha = 0.001$. In this particular example, $\alpha(0) = 5$ deg and $\alpha'(0) = \xi(0) = \xi'(0)$, but the initial conditions are not important in the calculation of system invariants. A sufficient embedding dimension of four was obtained using the percentage of false nearest neighbors, and the phase space was reconstructed. Eigenvalues of Jacobian matrices were calculated using the mapping technique already described, and average eigenvalues were evaluated. The nondimensional frequency and damping ratios obtained using the average eigenvalues of the Jacobian matrices are as follows:

$$\omega_1 \approx 0.2, \qquad \omega_2 \approx 1.16, \qquad \zeta_1 \approx 0.011, \qquad \zeta_2 \approx 0.002 \tag{19}$$

Modal damping and frequencies of the already given system were also calculated from the eigenvalues analysis of Eq. (18) giving

$$\omega_1 = 0.1990, \qquad \omega_2 = 1.1606$$

$$\zeta_1 = 0.00985, \qquad \zeta_2 = 0.00176 \tag{20}$$

Comparison of these values [Eq. (20)] with those estimated using the phase-space reconstruction technique [Eq. (19)] shows that the estimated values are very close to the exact values. The estimated values for frequency are good, and they do not change much with parameters such as time delay and the Taylor series order n_0. However, these parameters could substantially change the damping values. For example, a first-order expansion ($n_0 = 1$) gave a damping value of $\zeta_1 \approx 0.011$, but for a second-order expansion ($n_0 = 2$), a damping value of $\zeta_1 \approx 0.02$ was obtained. For this reconstructed phase space, the curvature of the Taylor series with n_0 of 2 or 3 can reasonably follow the curvature of the local data points, and $n_0 = 2$ or 3 should be appropriate in this case. However, the robustness of the results is of more concern here than proper selection of parameters such as the expansion order. The method could be improved such that the results are less sensitive to the parameters, and further studies are in progress.

Similar analyses have also been carried out for the two-degree-of-freedom aeroelastic system with and without the structural nonlinearities. For example, consider a linear system $M(\alpha) = \alpha$ with the following parameters: $U^*/U_L^* = 0.8$, $\mu = 100$, $a_h = -0.5$, $x_\alpha = 0.25$, $r_\alpha^2 = 0.25$, $\bar{\omega} = 0.8$, and $\zeta_\alpha = \zeta_\xi = 0.01$. At an airspeed of $U^*/U_L^* = 0.8$, the eigenvalues were determined using standard flutter analysis techniques[13] and yielded the following frequency and damping values:

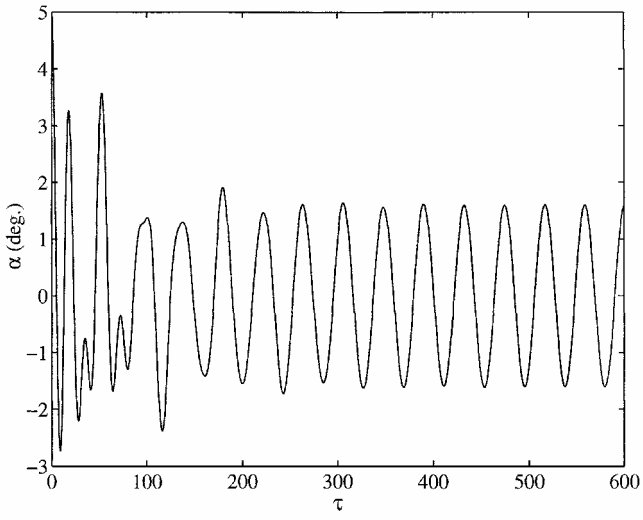

Fig. 10 Pitch motion of a linear two-dimensional airfoil: $U^*/U_L^* = 0.8$, $\mu = 100$, $a_h = -0.5$, $x_\alpha = 0.25$, $r_\alpha^2 = 0.25$, $\bar{\omega} = 0.8$, $\zeta_\alpha = \zeta_\xi = 0.01$, $\alpha(0) = 5$ deg, and $\alpha'(0) = \xi(0) = \xi'(0)$.

$$\omega_1 = 0.2425, \qquad \omega_2 = 0.3512$$

$$\zeta_1 = 0.0467, \qquad \zeta_2 = 0.0596 \tag{21}$$

If the airfoil is given a sinusoidal excitation with a nondimensional frequency of 0.1502, the time history of pitch angle is as shown in Fig. 10. The motion is started from rest with initial conditions $\alpha(0) = 5$ deg and $\alpha'(0) = \xi(0) = \xi'(0)$. When the mutual information and percentage of false nearest neighbors techniques are used, a phase space was reconstructed from the α motion. The eigenvalues of the mapping were calculated, and the frequency and damping values were estimated from the average mapping. For an embedding dimension of six, the frequency and damping values were estimated as follows:

$$\omega_1 \approx 0.1502, \qquad \omega_2 \approx 0.2432, \qquad \omega_3 \approx 0.3512$$

$$\zeta_1 \approx 0.0012, \qquad \zeta_2 \approx 0.0494, \qquad \zeta_3 \approx 0.0613 \tag{22}$$

When these estimated frequency and damping values are compared with those obtained via analytical techniques given in Eq. (21), it is clear that the frequency estimations are excellent and the damping values are reasonably good. Also note that not only the airfoil modal frequencies but also the excitation frequency are obtained with this method. The excitation mode is denoted by mode 1. The damping value associated with the excitation should be zero, but the estimated value is finite, though very small.

Parameters such as Taylor expansion order n_0 and time delay T have larger effects on the damping estimates than on the frequencies. Special attention must be exercised in selecting the best values for parameters such as n_0 and T. The embedding dimension is also very important. If too small an embedding dimension is chosen, then one of the aeroelastic modes will be lost, and the error in the other aeroelastic mode will be increased considerably.

The preceding technique of parameter identification was also employed for the airfoil with a cubic nonlinearity in pitch excited by a sinusoidal input. The cubic nonlinearity is given by $M = \alpha + 3\alpha^3$, which is a small deviation from linear stiffness for $-0.2 < \alpha < 0.2$ rad(± 12 deg). The estimated frequency and damping values for this case are as follows:

$$\omega_1 \approx 0.1514, \qquad \omega_2 \approx 0.2457, \qquad \omega_3 \approx 0.3506$$

$$\zeta_1 \approx 0.0059, \qquad \zeta_2 \approx 0.0666, \qquad \zeta_3 \approx 0.0569 \tag{23}$$

When the magnitude of the cubic nonlinearity term is increased, the uncertainty in the mean eigenvalues of the mapping is increased significantly. As a result, the frequency and damping values now show considerable disagreement with those obtained. This problem becomes even more severe when the method is applied to the system with bilinear nonlinearity. The results obtained for nonlinear cases suggest that, for systems with a small departure from linearity, this method is able to obtain reasonable estimates of frequency and damping ratios.

Conclusions

The signal processing tools commonly used to analyze flight flutter test data usually work very well for linear signals. However, it has been recognized that a source of difficulty in extracting flutter parameters, such as frequency and damping, is the nonlinear behavior of aircraft structural components. A phenomenon that can take place in the presence of nonlinearities is a randomlike response of the aircraft known as chaos. The time series of such signals bear some resemblance to deterministic signals corrupted with noise. Without recognizing the chaotic behavior of the signal, one may inadvertently use linear signal processing techniques to calculate the frequency and damping values of the flutter modes. This can lead to misleading results. More suitable methods based on tools developed for nonlinear dynamic systems can be used to extract parameters to describe the system behavior properly. The application of these techniques to aeroelasticity is still in its infancy stage. The method outlined is potentially useful to analyze nonlinear aeroelastic signals, but further studies are necessary to address the issues of noise and selection and optimization of the various parameters used in the method.

Acknowledgments

The authors gratefully acknowledge the financial support of Natural Sciences and Engineering Research Council of Canada. The first author would also like to acknowledge the guidance given by S. J. Price of McGill University.

References

[1]Lee, B. H. K., Price, S. J., and Wong, Y. S., "Nonlinear Aeroelastic Analysis of Airfoils: Bifurcation and Chaos," *Progress in Aerospace Sciences*, Vol. 35, No. 3, 1999, pp. 205–334.

[2]Abarbanel, H. D. I., *Analysis of Observed Chaotic Data*, Springer-Verlag, New York, 1996.

[3]Lee, B. H. K., and Wong, Y. S., "Neural Network Parameter Extraction with Application to Flutter Signals," *Journal of Aircraft*, Vol. 35, No. 1, 1998, pp. 165–168.

[4]Gallager, R. G., *Information Theory and Reliable Communication,* Wiley, New York, 1968.

[5]Abarbanel, H. D. I., Brown, R., Sidorowich, J. J., and Tsimring, L. S., "The Analysis of Observed Chaotic Data in Physical Systems," *Reviews of Modern Physics,* Vol. 65, No. 4, 1993, pp. 1331–1392.

[6]Fraser, A. M., and Swinney, H. L., "Independent Coordinates for Strange Attractors from Mutual Information," *Physical Review A*, Vol. 33, No. 2, 1986, pp. 1134–1140.

[7]Kennel, M. B., Brown, R., and Abarbanel, H. D. I., "Determining Embedding Dimension for Phase-Space Reconstruction Using Geometrical Construction," *Physical Review A: General Physics*, Vol. 45, No. 6, 1992, pp. 3403–3411.

[8]Briggs, K., "An Improved Method for Estimating Lyapunov Exponents of Chaotic Time Series," *Physical Letters A*, Vol. 151, No. 1, 1990, pp. 27–32.

[9]Bryant, P., Brown, R., and Abarbanel, H. D. I., "Lyapunov Exponents from Observed Time Series," *Physical Review Letters*, Vol. 65, No. 6, 1990, pp. 1523–1526.

[10]Brown, R., Bryant, P., and Abarbanel, H. D. I., "Computing the Lyapunov Spectrum of a Dynamical System from an Observed Time Series," *Physical Review A: General Physics*, Vol. 43, No. 6, 1991, pp. 2787–2806.

[11]Oseledec, V., "A Multiplicative Ergodic Theorem. Lyapunov Characteristic Numbers for Dynamical Systems," *Transactions of the Moscow Mathematical Society*, Vol. 19, 1968, pp. 197–231.

[12]Wolf, A., Swift, J. B., Swinney, H. L., and Vastano, J. A., "Determining Lyapunov Exponents from a Time Series," *Physica* D, Vol. 16, No. 3, 1985, pp. 285–317.

[13]Fung, Y. C., *An Introduction to the Theory of Aeroelasticity*, Dover, New York, 1993, pp. 186–240.

[14]Jones, R. T., "The Unsteady Lift of a Wing of Finite Aspect Ratio," NACA Rept. 681, 1940.

[15]Alighanbari, H., and Price, S. J., "The Post-Hopf-Bifurcation Response of an Airfoil in Incompressible Two-Dimensional Flow," *Nonlinear Dynamics*, Vol. 10, No. 4, 1996, pp. 381–400.

[16]Alighanbari, H., and Hashemi, S. M., "Bifurcation Analysis of an Airfoil Containing a Cubic Structural Nonlinearity and Subjected to Two-Dimensional Incompressible Flow," AIAA Paper 2002-1206, April 2002.